JOURNAL OF Materials CHEMISTRY

Calcination of the MCM-41 mesophase: mechanism of surfactant thermal degradation and evolution of the porosity

Matthew T. J. Keene,[a] Regis D. M. Gougeon,[b] Renaud Denoyel,[a] Robin K. Harris,[b] Jean Rouquerol[a] and Philip L. Llewellyn[a]

[a]*Centre de Thermodynamique et de Microcalorimétrie du CNRS, 26 rue du 141ème RIA, 13331 Marseille, Cedex 3, France. E-mail: pllew@ctm.cnrs-mrs.fr*
[b]*Department of Chemistry, University of Durham, South Road, Durham, UK DH1 3LE*

Received 21st June 1999, Accepted 16th September 1999

Sample controlled thermal analysis (SCTA) has been used to carefully and reproducibly eliminate the organic surfactant template from pure silica mesoporous MCM-41. The reproducibility allowed a number of intermediate species to be isolated permitting complementary measurements. To understand the mechanisms by which the surfactant is removed, evolved gas analysis as well as ^{1}H and ^{13}C MAS NMR were used. The liberation of the porosity and evolution of the surface hydrophobicity were followed by gas adsorption, XRD and immersion microcalorimetry.

It would seem that two types of cetyltrimethylammonium surfactant exist in the confined state, of which the large majority decomposes at a lower temperature (up to 200 °C) within the silica organic host than in the pure state. A small quantity of organic fragments are still observed within the pore structure up to 500 °C. Gas adsorption shows a pore blocking effect occurs during the surfactant removal.

Introduction

The structure of the mesoporous molecular sieve, MCM-41, comprises a uniform extended hexagonal pore arrangement.[1,2] This structure results in the material possessing a large BET surface area, a high porosity and a narrow pore size distribution that can be controlled by the selection of both the synthesis conditions and, moreover, the carbon chain length of the surfactant used. The pore sizes of these materials have been shown to be adjustable from 1.6 to 10.0 nm.

A wide variety of potential applications for these materials are under current investigation, such as those mentioned in ref. 3 which are as wide ranging as catalysis, host–guest chemistry, adsorption and membrane science. It would therefore seem important to understand the mechanisms of formation of such materials to be able to fine-tune the preparative conditions with regard to the desired application. With comparison to the numerous studies that have investigated the synthesis of these materials, little has been reported as to the mechanism by which the surfactant is removed from the mesophase.[4–7] However this step can considerably alter the final properties of the material. A number of methods for removing the organic phase exist, such as supercritical extraction,[8] solvent extraction[4,9,10] and ozone extraction.[11] However, the most common method employed for the removal of the organic template has been by thermal extraction or calcination. The reported conditions for calcination have been found to vary widely.[2,10]

In the present study sample controlled thermal analysis (SCTA)[12] is used to investigate the mechanism of pore emptying. This less conventional method is initially compared with standard linear thermogravimetric analysis. Using a linear heating rate there is little control over the thermal reactions that take place. This can, potentially, create significant pressure gradients that may have an effect on the structure of the sample.

Using SCTA a direct and continuous feedback from the reaction is used to control the heating program for the material.[12] In this way a controlled rate of elimination of the fragments from the organic template is obtained. This control permits both temperature and pressure gradients within the sample to be minimised and allows an increased differentiation between reaction steps. It is also possible to couple the SCTA apparatus to a mass spectrometer allowing the evolved gases to be studied *in situ* during the thermal decomposition of the organic template, cetyltrimethylammonium bromide (CTABr) within the silica framework. An excellent reproducibility can thus be obtained allowing intermediate samples to be isolated and characterised. In the present study, solid state MAS NMR studies of the intermediate materials have been used to give further insight into the breakdown of the surfactant structure as the temperature of mesophase calcination was increased. Variations in the porosity, wall thickness and surface hydrophobicity were investigated using nitrogen adsorption, powder X-ray diffraction (XRD) and immersion calorimetry. By using these complementary techniques a great deal of information can be obtained at the different steps of thermal decomposition of the surfactant.

There have been many adsorption studies previously carried out on MCM-41,[13–16] no study, to our knowledge, has investigated the changes to the porosity as the organic phase is thermally removed from the inorganic phase. This step, however, may prove to be essential for the preparation of well-defined mesoporous hybrid materials with different surface properties.

Gas adsorption studies of the MCM-41 materials[13–16] permit an estimation of the specific surface area, pore volume and average pore sizes. XRD, however, measures the periodicity of the pore structure. The pore wall thickness can be determined for these materials by subtracting the previously determined pore size from the XRD *a* value (distance between the centres of two pores).

Additionally immersion microcalorimetry was used to carry out an initial study of the surface chemistry of the intermediate materials. From the information gained, the effects of the thermal degradation of the surfactant on the porosity and hydrophobicity of the silica mesophase could be monitored.

The comparison of the results is used to postulate a mechanism for the thermal removal of the organic phase for

the formation of MCM-41. The evolution of the porosity during this template extraction is also highlighted.

Experimental

Surfactant silica mesophase preparation

The synthesis used is based on that proposed by Grün *et al.*[17] The quaternary ammonium salt, cetyltrimethylammonium bromide (CTABr, $CH_3(CH_2)_{15}N(CH_3)_3Br$; 2.40 g) from Aldrich was dissolved in distilled water (120 cm^3). Once the surfactant had all dissolved ammonia solution (8 cm^3; Merck, 32%) followed by tetraethyl orthosilicate (TEOS; 10 cm^3) from Aldrich (98%) were added. The solution was stirred for 60 min during which time a white precipitate was formed.

The precipitate was recovered by suction filtration and washed using distilled water (150 cm^3). After a further period of suction filtration (10 min), the mesophase was air-dried for a month before thermal treatment to try and maximise the silica wall condensation.[18]

Simultaneous thermogravimetric analysis and differential thermal analysis (TG/DTA)

The effects of heating the surfactant silica mesophase at a linear rate were investigated by thermal analysis using simultaneous thermogravimetric analysis and differential thermal analysis (TG/DTA). The sample (15 mg) was analysed using a Stanton Redcroft STA1000 at a heating rate of 10 °C min^{-1} in static air using recalcined alumina as the DTA reference.

Sample controlled thermal analysis (SCTA)

The SCTA experiments were carried out on an instrument described previously.[12,19] The experiments were carried out on *ca.* 70 mg samples at a rate of 0.14 mg h^{-1} and under a residual pressure of 5×10^{-3} mbar. Intermediate products were obtained by treating separate samples, from the same initial batch, up to 50, 100, 150, 175, 300, 480, 550, 760, and 1000 °C. *In situ* analysis of the evolved vapour phase was carried out using a quadrupole mass analyser (VG quadrupoles) with a maximum detection of $m/z = 100$.

Evolved gas analysis: gas chromatography coupled with mass spectrometry (GC/MS)

As a verification of the evolved gases observed using SCTA, an independent measurement was carried out at the Central Analysis Services of the CNRS at Vernaison (France). In this experiment, the mesophase was heated to 100 °C for 5 min during which time the evolved gases were collected in a cold trap at −180 °C. These evolved gases were then passed into a gas chromatography column with a quadrupole mass analyser (up to $m/z = 800$). The results were treated with comparison to pre-recorded spectra.

MAS NMR

^{1}H MAS NMR experiments were performed on a Chemagnetics CMX200 spectrometer, operating at 200.13 MHz, equipped with a Chemagnetics H,F probe and 4 mm zirconia Pencil rotors. The MAS rate was 12 kHz. The 90° pulse duration was 5 μs. The chemical shifts were referenced by replacement to the signal for tetramethylsilane and the relaxation delay was taken between 3 and 5 seconds.

^{13}C MAS spectra were recorded at 75.43 MHz on a Varian Unity Plus spectrometer. For ^{13}C MAS spectra, a 90° pulse duration of 4.5 μs and relaxation delays of between 14 and 30 s were used. In the cross-polarisation experiments, the Hartman–Hahn matching was set so that both the proton and carbon rf fields were equivalent to 55 kHz. The carbon chemical shifts were referenced to the high frequency peak of adamantane (38.4 ppm on the TMS scale). The intermediate materials used for the MAS NMR study were not dried or reheated prior to analysis.

Powder X-ray diffraction

The intermediate calcined mesophase samples were analysed by powder X-ray diffraction on a STOE Stadi P transmission X-ray diffractometer with a position sensitive detector (PSD) which was used for all analyses. The X-ray source was Cu-Kα radiation.

Isothermal adsorption–desorption

Static point-by-point nitrogen adsorption–desorption volumetry analyses (Omnisorp 100 Analyser, Coultronics, France) were carried out at 77 K on each of the samples produced by SCTA. The Brunauer–Emmett–Teller (BET) specific surface area, a, was calculated by taking the cross-sectional area of a nitrogen molecule as 0.162 nm^2. The total mesopore volume, V, was obtained by assuming that complete pore filling by the liquid condensate had occurred by $p/p^0 = 0.95$. For ideal cylindrical pores the pore radius, r, is related to the pore volume and the surface area by $r = 2V/a$.

Immersion microcalorimetry

The intermediate materials (approx. 0.015 g ≡ 20 m^2) were pretreated to remove any physisorbed water under vacuum (2×10^{-2} mbar, 2 days) before being sealed in a glass bulb with a brittle end sealed to a glass rod. The bulb was then placed in a conventional Tian–Calvet differential microcalorimeter with an immersion cell.[20,21] On depressing the glass rod, the brittle end was broken and the liquid, doubly deionised water, entered the bulb. The heat effects were then measured. A blank procedure was also carried out using an empty bulb in order that the heat effects from breaking the glass and the wetting of the bulb could be estimated.

Results

Simultaneous thermogravimetric analysis and differential thermal analysis (TG/DTA)

The TG curve obtained for the silica mesophase is similar to those previously published.[4,6] The linear heating of the silica mesophase shows that up to 120 °C about 5 wt% is lost. It appears from Fig. 1 that with continued heating to 300 °C there is an additional 30 wt% removed. At about 300 °C a slight reduction in the rate of weight loss is detected. This peak is

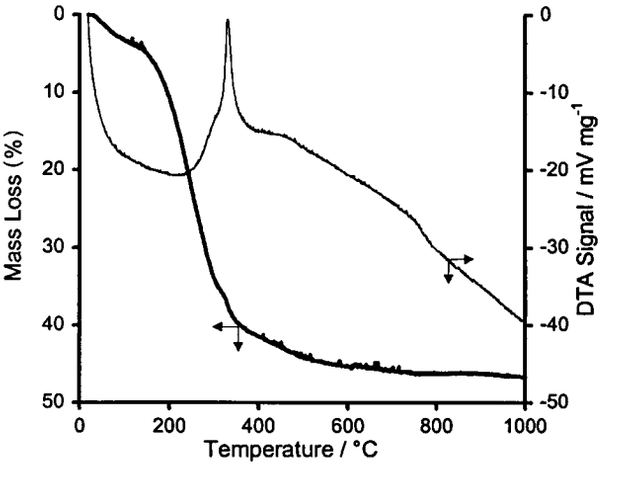

Fig. 1 Simultaneous TG/DTA of silica mesophase formed using cetyltrimethylammonium bromide (CTABr) surfactant.

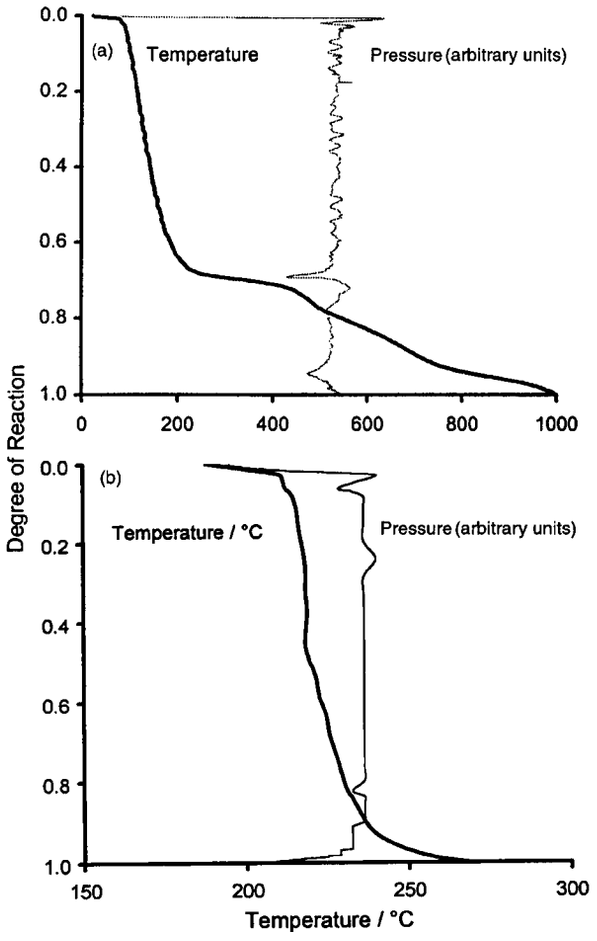

Fig. 2 Sample controlled thermal analysis (SCTA) of: (a) cetyltrimethylammonium bromide silica mesophase, and (b) pure CTABr.

associated with an exothermic signal. Subsequently, between 300 °C and 750 °C there is the further loss of 17 wt%.

Sample controlled thermal analysis (SCTA)

Sample controlled thermal analysis experiments were carried out on both the C_{16} silica mesophase [Fig. 2(a) and Fig. 3] and pure cetyltrimethylammonium bromide [Fig. 2(b)]. These curves are shown as the degree of reaction as a function of temperature. These temperature curves are thus equivalent to classic thermogravimetry curves, as the degree of reaction advancement is proportional to the weight loss for each individual step. The curves relating to the total pressure [Fig. 2(a)] or partial pressure (Fig. 3) are also given as a function of the degree of reaction advancement.

The SCTA curve [Fig. 2(b)] obtained with cetyltrimethylammonium bromide leads to a single step between 210 and 250 °C (under a residual pressure of 2×10^{-3} mbar and rate of 0.14 mg h^{-1}). Under the operating conditions, the evolved gas analysis shows principally the loss of $m/z = 14$, 15, 94 and 96. Small quantities of $m/z = 42$, 58, 79 and 81 are also observed.

The SCTA curve obtained with the C_{16} silica mesophase [Fig. 2(a)] shows a number of steps. The main step occurs between 100 and 220 °C, and corresponds to a mass loss of 30%. Further steps can be observed at higher temperatures: 450–550 °C and 650–750 °C. It can be seen that the total residual pressure above the sample remains relatively constant throughout the experiment.

Analysis of the evolved gases (Fig. 3) during the thermal treatment of the C_{16} silica mesophase shows a relatively complex picture. For ease of explanation, only a limited number of evolved masses are shown. The initial increase in temperature from 25 to 100 °C is characterised by the detection of $m/z = 18$, 17 and 16. These signals can be detected throughout the analysis.

From 100 to 195 °C, the mass analyser detects numerous signals that do not vary in ratio. A series of signals with a spacing of 14 can be distinguished ($m/z = 97$, 83, 69, 55, 41) as well as a number of other signals at $m/z = 15$, 18, 28, 29, 43 and 58. These results, as well as those obtained independently using the GC/MS set-up suggest the loss of hexadecene in this region.

From 195 to 220 °C, a variation in the ratio of mass signals occurs. In this region, a small but noticeable increase in mass signals of $m/z = 14$, 15, 94 and 96 is noted.

The steps in the SCTA curve from 450 to 550 °C and from 650 to 750 °C correspond to mass signals centred on $m/z = 15$, 16, 18 and 28 as well as weak signals corresponding of $m/z = 39$, 41 and 55. In the former step, the masses centred on $m/z = 18$ are dominant. The latter step is characterised by an increase in the masses centred on $m/z = 28$ as well as an increase in $m/z = 15$.

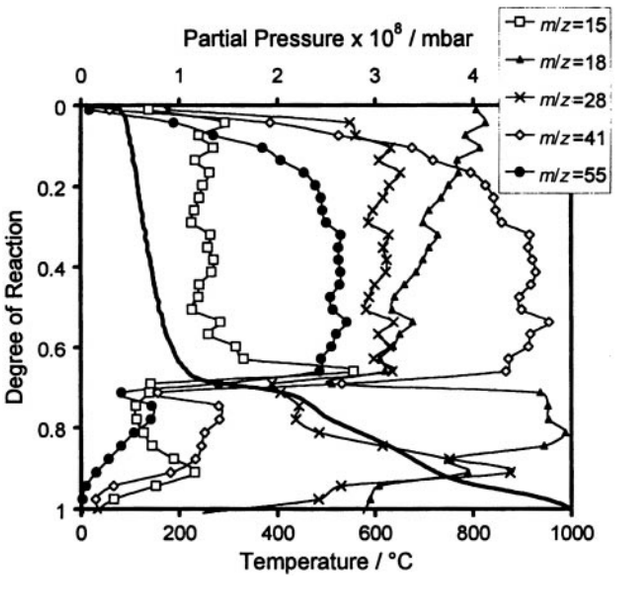

Fig. 3 SCTA coupled with evolved gas analysis (EGA) of the cetyltrimethylammonium bromide silica mesophase.

MAS NMR

Both ^1H and ^{13}C MAS NMR were used to study the intermediate samples thermally prepared by treating the pure silica mesophase.

Fig. 4 shows the ^1H NMR spectra of the intermediate

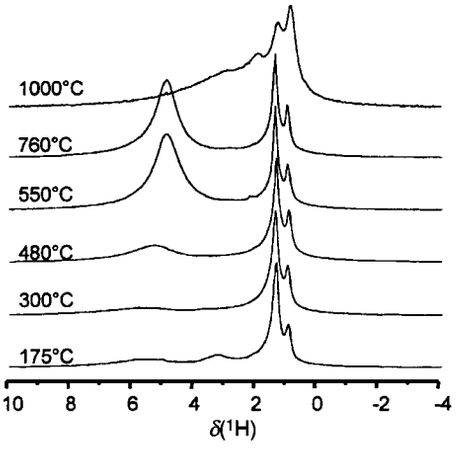

Fig. 4 ^1H MAS spectra of the silica mesophase intermediates heated by SCTA (16 transients for each spectrum).

samples treated *via* SCTA. Peaks at 0.92 and 1.34 ppm as well as a broad peak centred around 5 to 6 ppm are visible in each of the spectra of the intermediate samples treated up to 1000 °C. A peak at 3.30 ppm is visible on the spectrum of the sample treated to 175 °C, which disappears for the samples treated to higher temperatures.

Fig. 5 corresponds to the ^{13}C MAS NMR experiments. Several peaks can be observed in the spectrum obtained with the sample treated to 175 °C. These peaks are at relative shifts of 15, 24, 31, 33 and 54 ppm. The peak at 54 ppm disappears in the spectra of the samples treated to higher temperatures. For the sample treated to 550 °C, a distinct peak at 31 and maybe a second at 33 ppm are still observed. The peaks at 15 and 24 ppm may exist but are lost in the background noise.

Nitrogen adsorption

The nitrogen adsorption isotherm obtained with the sample treated up to 100 °C (Fig. 6) is a reversible straight line up to a relative pressure of 0.9. For the samples treated up to 150 °C and above, the isotherms are of Type IV character[22] with a distinct step in the region from $p/p^0 = 0.2$ to 0.35 according to the degree of surfactant removal. As the treatment temperature is increased,the inflection point of the step increases in p/p^0 (see also Fig. 7) and the width of the step decreases.

The desorption branch of the isotherm obtained with the intermediate treated to 150 °C does not close with the adsorption branch at low relative pressures. The isotherm obtained with the sample treated to 300 °C shows similar behaviour, although to a lesser extent. It is only after the sample is treated to 550 °C that the desorption branch closes to the adsorption branch. In this case, and with the samples treated to higher temperatures, no hysteresis is observed. The sample treated to 760 °C adsorbs almost 50% more gas than the material calcined to 300 °C. However, a 23% reduction in the nitrogen adsorption is found for the material treated to 1000 °C with respect to that treated to 760 °C.

From Fig. 7 the position of the p/p^0 inflection point is seen to move progressively up in pressure with increasing temperature. However, for the material that was calcined at 1000 °C, it can be seen that the position of the p/p^0 inflection point decreases to the value exhibited at 550 °C. The pore radii ($r = 2V/a$) have also been found to initially increase with temperature, from 0.67 nm for the sample heated to 150 °C to 1.27 nm at 175 °C. Although there is a further small increase in the pore size with further increasing temperature of thermal treatment, it can be seen that from 200 °C the pores formed do not significantly vary in size (about 1.4 nm).

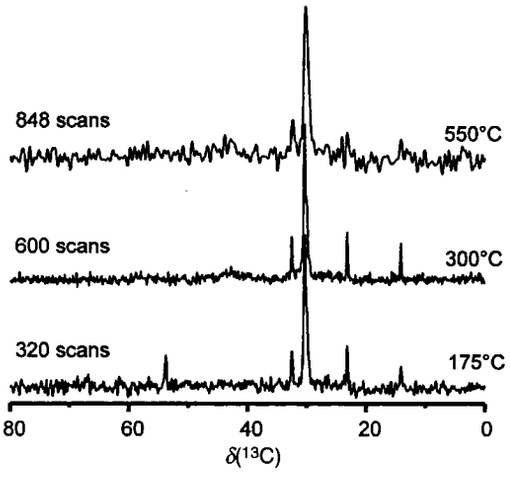

Fig. 5 ^{13}C MAS spectra of the silica mesophase intermediates thermally treated by SCTA (number of transients noted for each spectrum).

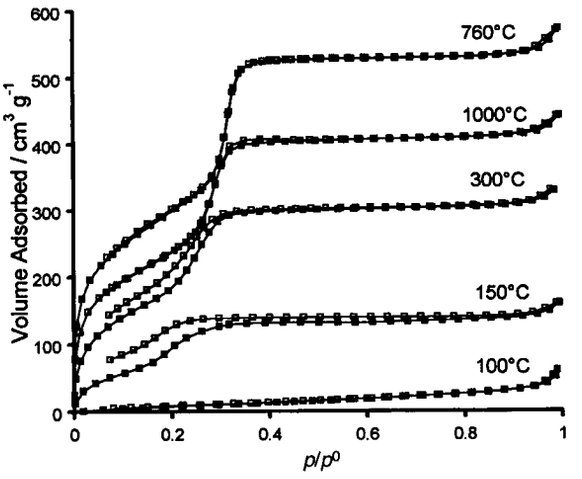

Fig. 6 Nitrogen adsorption–desorption isotherms of intermediate silica mesophases thermally treated at different temperatures *via* sample controlled thermal analysis.

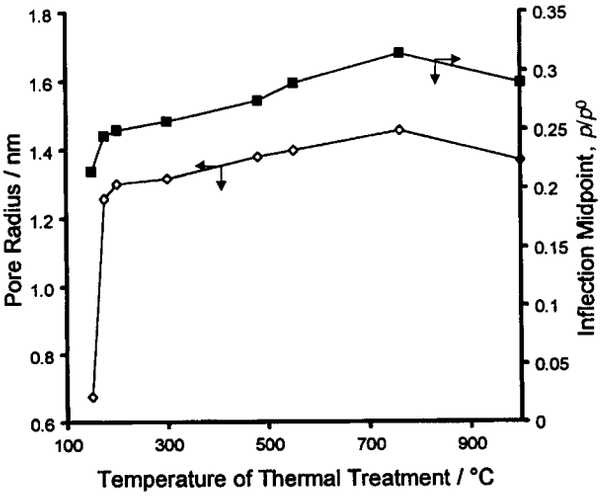

Fig. 7 Variation of p/p^0 midpoint in the nitrogen adsorption isotherm and pore size ($r = 2V/a$) for intermediate silica mesophase samples.

Powder X-ray diffraction

The powder X-ray diffraction pattern of the calcined mesophase samples shows that as the material is heated up to 150 °C the *d*-spacing diminishes. The d_{100} peak then remains constant up to 550 °C, at 3.95 nm. This gives $a = 4.56$ nm, and

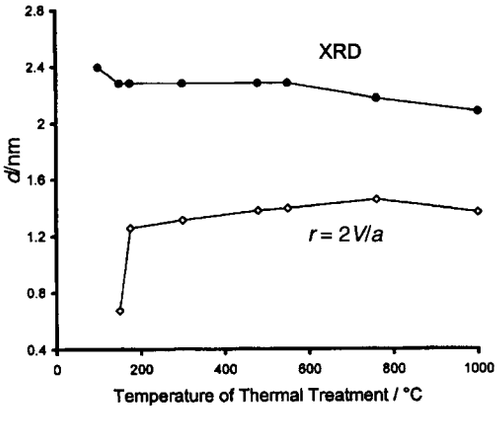

Fig. 8 Estimation of pore wall thickness from the pore size determined by nitrogen adsorption (diamonds) and from X-ray diffraction (circles).

thus a radius r ($=a/2$) of 2.28 nm (Fig. 8). It was found that thermally treating the sample to a higher temperature again caused the average size to decrease in width, $a=4.16$ nm ($r=2.08$ nm) for the material that is calcined at 1000 °C.

Immersion microcalorimetry

The enthalpy of immersion, ascertained by immersion microcalorimetry, increases as the temperature of the thermal treatment increases to 550 °C (-123 mJ m^{-2}; Fig. 9). Above this temperature the enthalpy of immersion for the material prepared at 760 °C decreases to -86 mJ m^{-2} whilst at 1000 °C there is a slight increase to -105 mJ m^{-2}.

Discussion

Thermal analysis

The overall shape of the SCTA curve [Fig. 2(a)] obtained with the silica mesophase material resembles the TG/DTA curve (Fig. 1). Nevertheless, the higher temperature steps (above 450 °C) are more distinct on the SCTA curve. This is due to the different operating conditions for each of the experiments.

Whereas the SCTA temperature curve obtained for the C_{16} silica mesophase [Fig. 2(b)] is characterised by several steps, the curve obtained for pure CTABr [Fig. 2(a)] only shows one step. Thus, the degradation of CTABr within the silica host is both different and more complex than in the pure state. Furthermore, the major step observed with the C_{16} silica mesophase (100–195 °C) occurs at a lower temperature than the step observed with pure CTABr (210–250 °C). This seems logical, as the CTABr within the silica host is amorphous, whereas bulk CTABr is crystalline.

Under SCTA conditions, the *pure CTABr* would seem to decompose *via* cleavage of the methyl groups to the nitrogen yielding CH_3Br ($m/z=94$ and 96). Only a small signal corresponding to the head group [$m/z=58$, $(CH_3)_2N{=}CH_2$] is observed. Signals corresponding to the C_{16} alkyl chain are not detected. This is most likely due to the experimental set-up with condensation of the alkyl chain at a cold point.

The *C_{16} silica mesophase* undergoes a far more complex decomposition. An initial loss of water ($m/z=18$, 17, 16), and maybe residual ammonia ($m/z=17$, 18) from the synthesis,[17] up to a temperature of 100 °C is observed. The production of water throughout the rest of the experiment would result from silanol condensation.

In the step *from 100 to 195 °C*, a number of species are detected in an unchanging ratio. From the series of masses observed ($m/z=97$, 83, 69, 55, 41, *etc.*) it would seem that an alkene is formed. This corresponds to the detection of hexadecene in the independent GC/MS experiments. As an alkene is formed, this may explain its detection here and not in the case of the experiment with pure CTABr where the surfactant tail may remain as the alkene. This latter point needs to be verified. A number of the other masses would seem to correspond to the surfactant head group ($m/z=15$, CH_3; $m/z=28$, C_2H_4; $m/z=29$, C_2H_5 and/or CH_3N; $m/z=43$, C_2N_5N; $m/z=58$, C_3H_8N).

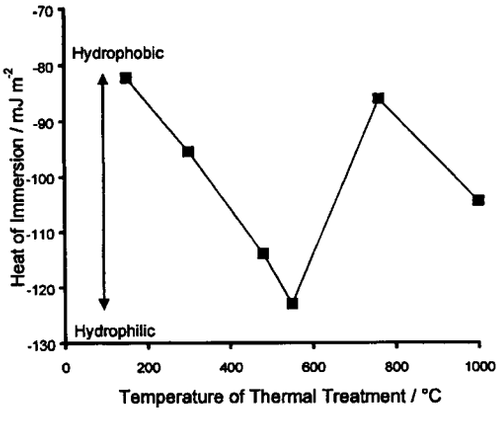

Fig. 9 Measure of hydrophobicity determined by immersion calorimetry of intermediate samples thermally treated *via* SCTA.

The MAS NMR results are similar to those previously obtained by Wang *et al.*[23] In their publication the carbons in the surfactant are numbered as follows:

$$\underset{C_{17}}{CH_3}\text{-}\underset{C_{16}}{CH_2}\text{-}\underset{C_{15}}{CH_2}\text{-}\underset{C_{14}}{CH_2}\text{-}\underset{C_{13}}{CH_2}\text{-}\underset{C_{12}}{CH_2}\text{-}\underset{C_{11}}{CH_2}\text{-}\underset{C_{10}}{CH_2}\text{-}\underset{C_{9}}{CH_2}\text{-}$$

$$\underset{C_{8}}{CH_2}\text{-}\underset{C_{7}}{CH_2}\text{-}\underset{C_{6}}{CH_2}\text{-}\underset{C_{5}}{CH_2}\text{-}\underset{C_{4}}{CH_2}\text{-}\underset{C_{3}}{CH_2}\text{-}\underset{C_{2}}{CH_2}\text{-N-}\underset{C_{1}}{(CH_3)_3}$$

The ^{13}C MAS NMR spectrum obtained with the intermediate product treated to 175 °C (Fig. 5) thus reveals the presence of the C_1 carbon at 54 ppm, C_4–C_{14} at 31 ppm, C_{15} at 33 ppm, C_{16} at 24 ppm and C_{17} at 15 ppm. However, it is interesting to note that signals relating to the C_2 (68 ppm) and C_3 (27 ppm) carbons are not observed. This is not inconsistent with the cleavage of the head with the alkyl chain of the surfactant (see below). The loss of the peaks due to C_2 and C_3 may be due to the formation of an alkene as suggested by the evolved gas analysis (although no new NMR signals are seen).

The ^1H MAS NMR spectra (Fig. 4) of the various samples all show a rather broad peak at 5–6 ppm, which corresponds to a water resonance. The fact that this varies from sample to sample can be explained by the lack of particular storage precautions after sample preparation. The ^1H MAS NMR spectrum of the sample treated to 175 °C shows two major signals at 0.92 and 1.34 ppm which are attributable to C_{17} and C_4–C_{15} carbons respectively. Unfortunately, it is difficult to obtain information on the CH_2/CH_3 ratio from a deconvolution of these peaks as they may also contain information from a resonance of the silica silanols. A signal is observed at 3.30 ppm, which corresponds to the C_1 carbon.[24] This corresponds well with the C_1 signal observed in the ^{13}C spectrum. It would thus seem that the nitrogen–C_1 carbon head group is still present in some quantity within the pores of the silica host at this temperature.

In the region *from 195 to 220 °C*, the lack of any distinct variation in the SCTA temperature curve may be explained by only a slight modification in surfactant decomposition. As the evolved gas analysis (Fig. 3) shows the continuing loss of masses due to the surfactant head group (*e.g.* $m/z=58$, 43) and chain (*e.g.* $m/z=55$, 41, *etc.*) it would seem that the processes that occur from 100 to 195 °C persist. However, the increase in peaks due to CH_3Br ($m/z=94$, 96, 15) would seem to indicate the loss of a small amount of surfactant decomposed *via* a second mechanism. A crude estimation suggests that this corresponds to around 5% of the surfactant, probably as CTABr. It is rather surprising to observe that there are any bromine species at all as one would expect excess CTABr to be washed away after the synthesis. However, as the powder was washed to pH = 7, one would expect there to be no excess CTABr on the surface of the sample. Furthermore, chemical analysis of the sample before calcination also suggests a small amount of bromide species present. It would thus seem possible for a small amount of the CTABr to rest within the micelles without exchange with the silica species during the synthesis. What is surprising in this case is that this is not eliminated earlier in the thermal degradation process. However, it is in this region of temperature that the pure surfactant decomposes. It would thus seem that some of the surfactant may decompose in an analogous manner to the pure surfactant giving the signals ($m/z=15$, 94 and 96).

Information pertaining to the species left within the silica mesopore structure after the main decomposition is obtained from the MAS NMR spectra (Fig. 4 and 5) of the intermediate sample *treated to 300 °C*. It can be clearly seen in both the ^{1}H and ^{13}C spectra that signals due to the surfactant chain are still present. However, signals due to the C_1 carbon are no longer visible. In ^{13}C CP-MAS spectra (not shown), two signals at 43 and 56 ppm appear (the latter at not much above the noise level) for the sample treated to 300 °C whereas the signal at 54 ppm disappears. These signals are thought to correspond to a dimethyl group and $N–CH_2$ of an amine whilst the signal at 54 ppm corresponds to the C_1 carbon of the surfactant.[24] It thus seems that some organic species remain within the mesopores after the main mass loss up to 220 °C. Although readsorption of the decomposition products is possible, it seems unlikely under the experimental conditions used (residual pressure of 2×10^{-3} mbar and rate of 0.14 mg h^{-1}). This would suggest that some of the decomposition species produced react with the silica surface during decomposition or that a portion of the surfactant is relatively strongly bound to the surface during the synthesis.

In the steps *from 450 to 550 °C* and *from 650 to 750 °C*, the weak signals at $m/z = 55, 41, 39$ as well as the signals centred on $m/z = 28$ indicate the continued loss of small quantities of carbon tail fragments (Fig. 3). In these regions, a significant amount of water is still also lost. The ^{1}H (Fig. 4) and ^{13}C MAS NMR (Fig. 5) spectra of the samples treated above 550 °C all indicate some persistence of carbon chain fragments, although in similar quantities with increasing temperature.

Pore volume

The thermal removal of the surfactant from the mesophase is seen to have an effect on the nature and extent of the porosity of the material produced (see Fig. 6–8). At low temperatures (below 150 °C), where it is believed that the surfactant is removed *via* cleavage to give hexadecene and an amine, there is no mesoporosity detected, however from the *t*-plot no microporosity was found either.

Mesoporosity is first found when the material is thermally treated to 150 °C. However, with the isotherm for the mesophase heated to 150 °C, unlike most reported isotherms, the desorption branch does not return to the adsorption branch. This indicates that not all of the probe gas is removed at low pressure from these materials. Continued heating of the mesophase can be seen from Fig. 7 to increase the volume of gas adsorbed, but still the desorption branch is clearly detached from the adsorption curve. It is only once the mesophase has been thermally treated to 550 °C that the adsorption branch is rejoined after the hysteresis. Since this effect is resolved by increased heating it is unlikely to be the pore shape that is hindering the desorption of the gas. A possible explanation for this is that some of the nitrogen is trapped within the porosity. Until the mesophase is heated above 550 °C, the pores still contain surfactant molecules, thus the probe gas may become trapped between the alkyl tail chains of these molecules.

The pore volume was found to almost double from 150 to 300 °C and then again as the temperature of the calcination increased to 760 °C. However, the mass losses measured after SCTA for these two temperature regions were found to be about 50 and 25% respectively. It is thought, for this reason in conjunction with the desorption branch not returning to the adsorption branch, that some pore blocking is taking place. This is more clearly illustrated in Fig. 10 where the SCTA temperature curve is plotted in conjunction with the percentage of pore volume liberated as determined from the nitrogen adsorption isotherms. One would expect that the pore volume liberated would be proportional to the loss of surfactant (SCTA curve); as can be seen up to 200 °C and above 550 °C, this is the case. However in the region between 200 °C and 550 °C, some of the pore volume is not able to be accessed using nitrogen adsorption.

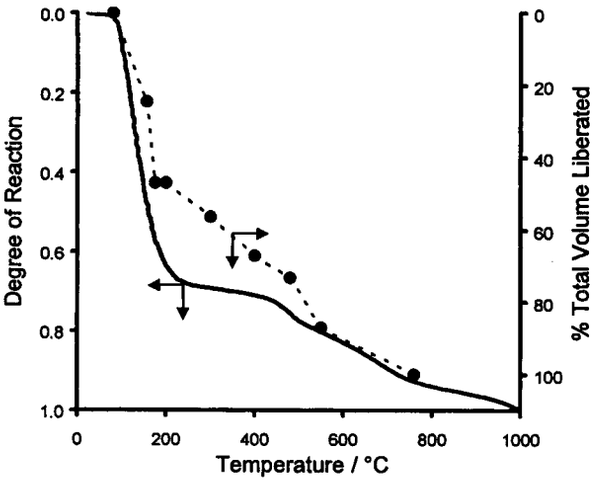

Fig. 10 Comparison of the SCTA curve, relating to the extent of reaction, and the % of the total pore volume liberated.

It is suggested that two types of surfactant exist in the as-synthesised mesophase. It may be that those which are more strongly bound to the silica surface could act as barriers and/or as valves during the gas adsorption measurements. Thus some of the porosity is completely blocked. However, some of the probe molecules may be able to enter the pores but are prevented from being removed at low pressures, as is indicated by the non-return of the desorption branch. A simple picture of the pore structure for the intermediates may be to consider that the mesopores are at least partially blocked by some surfactant residues. This porosity entraps the portion of the probe gas which is responsible for the hysteresis.

Pore width

The p/p^0 inflection points on the adsorption branches (Fig. 7) are seen to increase as the temperature of mesophase heating increases. This can be used to show the evolution of the pore size. After a relatively large jump from 150 °C to 175 °C, only a small increase in inflexion point occurs up to 760 °C. However, heating the mesophase to 1000 °C is seen to decrease the position of the p/p^0 inflection point compared to the position for the material heated to 760 °C. This is the same region of calcination (760 to 1000 °C) when the pore volume is found to decrease significantly. This most likely results from structure breakdown at 1000 °C. This is confirmed by the X-ray analysis where a clear degradation of the pattern is observed for this latter sample.

Another interesting test for this 'model' type of mesoporous material, believed to exhibit cylindrical channels, is the relationship $r = 2V/a$. Although no microporosity is observed from the lack of Type I behaviour in the isotherm obtained for the sample heated to 150 °C (Fig. 6), an average pore radius of 0.67 nm is calculated using this relationship (Fig. 8). This may be due to a poor estimation of V or a. From 175 (1.27 nm) to 200 °C (1.40 nm) a small increase was found but after this temperature the average pore radius was not found to change on further heating of the sample.

Pore wall thickness

The X-ray diffraction patterns of the materials thermally treated by SCTA show that as the surfactant mesophase is heated to 150 °C there is a small shrinkage in the *d*-spacing (see Fig. 8). This is consistent with the sample shrinking on drying due to increased polycondensation of the silanol groups. The *d*-spacing on heating the mesophase to 550 °C is then found to be constant at 3.95 nm ($r = 2.28$ nm). Further calcination at high

temperatures is found to decrease the *d*-spacing by about 0.1 nm for each further 200 °C.

The values obtained for the pore radii from gas adsorption combined with the *d*-spacings found by XRD can be used to estimate the thickness of the pore wall (Fig. 8). This is about 2.0 nm at 550 °C. However, by increasing the temperature above 500 °C the pore walls are found to thin slightly to 1.8 nm at 760 °C. This is a relatively large value when compared to that often cited in the literature[2,7] and may be due to the particular experimental synthesis and calcination conditions used.

Surface properties

The surface of the silica was investigated using immersion microcalorimetry with water to study the hydrophobicity of the sample (Fig. 9). One way to define the hydrophilic or hydrophobic character of a surface is to compare the immersion enthalpy to that of the superficial enthalpy of the liquid/vapour interface, this is 118 mJ m^{-2} in the case of water at 25 °C (above 118 mJ m^{-2}, the surface is considered hydrophilic).[25]

On heating, most amorphous silicas lose hydroxy groups and thus become more hydrophobic up to 1000 °C.[26] The present study shows a slightly more complicated picture with the presence of organic molecules within the pores. This would explain the increasing hydrophilicity up to 550 °C where progressive loss of the hydrophobic effects of the alkyl chains occurs. Once all of the organic molecules are lost at 550 °C, the expected behaviour of increasing surface hydrophobicity occurs up to 750 °C. This results from silanol condensation which is the reason that water is detected at high temperatures during the calcination of the mesophase. Breakdown of the MCM-41 pore structure around 1000 °C creates defects that are hydrophilic in nature, causing the slight increase in the enthalpy seen at this temperature in Fig. 9.

Conclusions

The present study was aimed to understand the mechanism of cetyltrimethylammonium surfactant calcination from a pure silica mesophase using sample controlled thermal analysis. It would seem that the surfactant is present in two forms within the inorganic host: the majority which is relatively loosely bound and a small quantity of more strongly bound species.

The majority of the surfactant breaks down in the region from 100 to 220 °C, to form hexadecene and a trimethylamine species. This surfactant breaks down at a lower temperature than in the pure state, as a result of the amorphous and/or confined state of the organic species.

The direct formation of the mesoporosity occurs without prior formation of microporosity. This does not exclude the possibility that micropores may form at the channel entrances which retain the nitrogen on desorption even though this microporous volume is negligible. This, along with diffusion of nitrogen between surfactant chains, would explain the unusual hysteresis phenomena observed. The surface that is available on heating the sample in this region is notably hydrophobic. The mesopore mean size that is observed, however, is almost the same as in the finally calcined product at 760 °C.

From 195 to 220 °C, a second mechanism of surfactant loss superimposes on the first, which would seem to be due to species more strongly bound to the silica surface. This small quantity of surfactant breaks down *via* a mechanism analogous to the thermal decomposition of the pure surfactant under the same experimental conditions.

Several species derived from the organic surfactant would seem to remain within the inorganic host. It is suggested that these species are bound to the silica surface and are eliminated in the steps occurring at higher temperatures (450–550 °C and 650–750 °C). This may be associated with the pore blocking effect that extends up to 550 °C.

In the temperature region from 200 °C to 550 °C, the surface available becomes more hydrophilic. The most hydrophilic product is obtained at 760 °C. At this temperature, both the pore volume and the accessible surface area are at maxima. At higher temperatures, structure breakdown occurs.

Concerning the actual mechanism of surfactant degradation, a Hoffman degradation based mechanism is often proposed,[7] may be in analogy to tetrapropylammonium degradation within MFI-type zeolites.[27] Our results would seem to confirm such a mechanism for the majority of the surfactant species present. This would lead to the following reaction scheme:

$$\underset{\text{Surface}}{\text{Si–O}^-} \; \underset{\text{CTA}}{^+\text{N(CH}_3)_3\text{CH}_2\text{CH}_2(\text{CH}_2)_{13}\text{CH}_3} \Rightarrow$$

$$\text{Si–OH} + \underset{\text{Trimethylamine}}{\text{N(CH}_3)_3} + \underset{\text{Hexadecene}}{\text{CH}_2{=}\text{CH(CH}_2)_{13}\text{CH}_3}$$

However a number of side reactions, notably with the silica surface, also occur. It is thus possible to imagine a mechanism based on the Cope elimination. Such reactions would explain the loss of certain species at reaction temperatures above 220 °C.

Acknowledgements

The authors acknowledge support received from the European Community within the scope of the MESOP network (TMR programme 95-98 contract no. ERB FM RX CT 960084). They also especially thank Dr P. Trens at the University of Reading for kindly carrying out the TG/DTA measurements.

References

1 J. S. Beck, J. C. Vartuli, W. J. Roth, M. E. Leonowicz, C. T. Kresge, K. D. Schmitt, C. T.-U. Chu, D. H. Olsen, E. W. Sheppard, S. B. McCullen, J. B. Higgins and J. L. Schlenker, *J. Am. Chem. Soc.*, 1992, **114**, 10 834.
2 C. T. Kresge, M. E. Leonowicz, W. J. Roth, J. C. Vartuli and J. S. Beck, *Nature*, 1992, **359**, 710.
3 See for example, various articles in *Stud. Surf. Sci. Catal.*, 1998, **117**.
4 R. Schmidt, D. Akporiaye, M. Stöcker and O. H. Ellestad, *Stud. Surf. Sci. Catal.*, 1994, **84**, 61.
5 A. Corma, V. Fornés, M. T. Navarro and J. Pérez-Pariente, *J. Catal.*, 1994, **148**, 569.
6 A. Montes, E. Cosenza, G. Giannetto, E. Urquieta, R. A. de Melo, N. S. Gnep and M. Guisnet, *Stud. Surf. Sci. Catal.*, 1998, **117**, 237.
7 S. Hitz and R. Prins, *J. Catal.*, 1997, **168**, 194.
8 S. Kawi and M. W. Lai, *Chem. Commun.*, 1998, 1407.
9 P. T. Tanev and T. J. Pinnavaia, *Chem. Mater.*, 1996, **8**, 2068.
10 X. S. Zhao, G. Q. Lu, A. K. Whittaker, G. J. Millar and H. Y. Zhu, *J. Phys. Chem. B*, 1997, **101**, 6525.
11 M. T. J. Keene, R. Denoyel and P. L. Llewellyn, *Chem. Commun.*, 1998, 2203.
12 J. Rouquerol, *J. Thermal Anal.*, 1989, **144**, 209.
13 R. Schmidt, M. Stöcker, E. Hansen, D. Akporiaye and O. H. Ellestad, *Microporous Mater.*, 1995, **3**, 443.
14 O. Franke, G. Schulz-Ekloff, J. Rathousky, J. Starek and A. Zunkal, *J. Chem. Soc., Chem. Commun.*, 1993, 724.
15 P. J. Branton, P. G. Hall and K. S. W. Sing, *J. Chem. Soc., Chem. Commun.*, 1993, 1257.
16 P. L. Llewellyn, Y. Grillet, F. Schüth, H. Reichert and K. K. Unger, *Microporous Mater.*, 1994, **3**, 345.
17 M. Grün, I. Lauer and K. Unger, *Adv. Mater.*, 1997, **9**, 254.
18 H. P. Lin, S. Cheng and C.-Y. Mou, *J. Chin. Chem. Soc.*, 1996, **43**, 375.
19 J. Rouquerol, S. Bordère and F. Rouquerol, *Thermochim. Acta*, 1992, **203**, 193.
20 S. Partyka, F. Rouquerol and J. Rouquerol, *J. Colloid Interface Sci.*, 1979, **68**, 21.

21 R. Denoyel, F. Rouquerol and J. Rouquerol, in *Fundamentals of Adsorption*, ed. A. J. Liapis, Engineering Foundation, New York, 1987, p. 199.
22 K. S. W. Sing, D. H. Everett, R. A. W. Haul, L. Moscou, R. A. Pierotti, J. Rouquerol and T. Siemieniewska, *Pure Appl. Chem.*, 1985, **57**, 603.
23 L.-Q. Wang, J. L. Liu, G. J. Exarhos and B. C. Bunker, *Langmuir*, 1996, **12**, 2663.
24 M. T. Janicke, C. C. Landry, S. C. Christiansen, D. Kumar, G. D. Stucky and B. F. Chmelka, *J. Am. Chem. Soc.*, 1998, **120**, 6940.
25 D. A. Spagnolo, Y. Maham and K. T. Chang, *J. Phys. Chem.*, 1996, **100**, 6626.
26 Y. Grillet and P. L. Llewellyn, in *The Surface Properties of Silica*, ed. A. P. Legrand, J. Wiley & Sons, Chichester, 1998, p. 60.
27 L. M. Parker, D. M. Bibby and J. E. Patterson, *Zeolites*, 1984, **14**, 168.

Paper 9/04937A